Intramolecular Ligand Hydroxylation: Mechanistic High-Pressure Studies on the Reaction of a Dinuclear Copper(I) Complex with Dioxygen

Michael Becker and Siegfried Schindler*

Institute for Inorganic Chemistry, University of Erlangen-Nürnberg, Egerlandstrasse 1, 91058 Erlangen, Germany

Kenneth D. Karlin*

Department of Chemistry, Johns Hopkins University, Baltimore, Maryland 21218

Thomas A. Kaden, Susan Kaderli, Tania Palanché, and Andreas D. Zuberbühler*

Institut für Anorganische Chemie, Universität Basel, Spitalstrasse 51, Switzerland

Received September 3, 1998

We provide a mechanistic study of a monooxygenase model system and detail low-temperature stopped-flow kinetics studies in acetone as solvent, employing both the use of rapid-scanning diode-array observation and variable high-pressure (20−100 MPa) techniques. The dicopper(I) complex employed is $[Cu_2(H\text{-}XYL\text{-}H)]^{2+}$ (**1**), with the H-XYL-H ligand wherein a *m*-xylyl group links two bis[2-(2-pyridyl)ethyl]amine units. This reacts with O_2 reversibly (k_1/k_{-1}) giving a peroxo−dicopper(II) intermediate $[Cu_2(H\text{-}XYL\text{-}H)(O_2)]^{2+}$ (**2**), which thereupon irreversibly (k_2) reacts by oxygen atom insertion (i.e., hydroxylation) of the xylyl group, producing $[Cu_2(H\text{-}XYL\text{-}O^-)(OH)]^{2+}$ (**3**). Activation parameters are as follows: k_1, $\Delta H^{\ddagger} = 2.1 \pm 0.7$ kJ/mol, $\Delta S^{\ddagger} = -174 \pm 3$ J/(K mol); k_{-1}, $\Delta H^{\ddagger} = 80.3 \pm 0.8$ kJ/mol, $\Delta S^{\ddagger} = 77 \pm 3$ J/(K mol); k_2, $\Delta H^{\ddagger} = 58.2 \pm 0.2$ kJ/mol, $\Delta S^{\ddagger} = -5.8 \pm 0.9$ J/(K mol). These values are similar to values obtained in a previous study in dichloromethane. At low temperatures and higher concentrations, the situation in acetone is complicated by a pre-equilibrium of **1** to an isomer form. The present study provides the first determination of activation volumes for individual steps in copper monooxygenase reactions. The data and analysis provide that $\Delta V^{\ddagger}(k_1) = -15 \pm 2.5$ cm^3/mol and $\Delta V^{\ddagger}(k_{-1}) = +4.4 \pm 0.5$ cm^3/mol for formation and dissociation of **2**, respectively, while $\Delta V^{\ddagger}(k_2) = -4.1 \pm 0.7$ cm^3/mol; a volume profile for the overall reaction has been constructed. The significance of the findings in the present study is described, and the results are compared to those for other systems.

Introduction

Copper monooxygenases catalyze a number of different reactions and include enzymes possessing varied active site structures.[1,2] Tyrosinase[2] possesses a dinuclear active site similar to that in hemocyanins[2] (arthropodal[3] and molluscan[4] blood O_2 carriers), where the reduced dicopper(I) site reacts with O_2 giving a μ-η^2:η^2-peroxo bridged dicopper(II) species (Cu···Cu ∼ 3.6 Å) capable of phenol substrate oxygenation (producing *o*-catechols, or *o*-quinones directly[5,6]). Dopamine β-monooxygenase (DβM) (benzylic hydroxylation; dopamine → norepinephrine) and the related peptidylglycine α-amidating monooxygenase (PAM) also require two copper ions per functional subunit;[1] an X-ray structure[7] of the latter reveals a methionine ligand present at the putative catalytic oxygenating Cu center, with Cu···Cu ∼ 11 Å. Evidence has been presented for the presence of clusters of copper ions at the active sites of bacterial particulate methane monooxygenase and ammonia monooxygenase enzymes.[2,8]

Chemical model systems for copper monooxygenases[9−11] are of interest in elucidating fundamental aspects of copper/dioxygen interactions, and for the potential to develop reagents or catalysts for selective organic oxidations.[12−14] In the past few years, considerable attention has been given to discrete dinuclear

(1) Klinman, J. P. *Chem. Rev.* **1996**, *96*, 2541−2561.
(2) Solomon, E. I.; Sundaram, U. M.; Machonkin, T. E. *Chem. Rev.* **1996**, *96*, 2563−2605.
(3) Magnus, K. A.; Hazes, B.; Ton-That, H.; Bonaventura, C.; Bonaventura, J.; Hol, W. G. J. *Proteins: Struct., Funct., Genet.* **1994**, *19*, 302−309.
(4) Cuff, M. E.; Miller, K. I.; van Holde, K. E.; Hendrickson, W. A. *J. Mol. Biol.* **1998**, *278*, 855−870.
(5) Cooksey, C. J.; Garratt, P. J.; Land, E. J.; Pavel, S.; Ramsden, C. A.; Riley, P. A.; Smit, N. P. M. *J. Biol. Chem.* **1997**, *272*, 26226−26235.
(6) Clews, J.; Cooksey, C. J.; Garratt, P. J.; Land, E. J.; Ramsden, C. A.; Riley, P. A. *Chem. Commun.* **1998**, 77−78.
(7) Prigge, S. T.; Kolhekar, A.; Eipper, B. A.; Mains, R. E.; Amzel, M. *Science* **1997**, *278*, 1300−1305.
(8) Elliott, S. J.; Randall, D. W.; Britt, R. D.; Chan, S. I. *J. Am. Chem. Soc.* **1998**, *120*, 3247−3248.
(9) Karlin, K. D.; Zuberbühler, A. D. In *Bioinorganic Catalysis*, 2nd ed.; Reedijk, J., Bouwman, E., Eds.; Marcel Dekker: New York, 1999, pp 469−534.
(10) Kopf, M.-A.; Karlin, K. D. In *Biomimetic Oxidations*; Meunier, B., Ed.; Imperial College Press: London; Chapter 7, in press.
(11) Karlin, K. D.; Tyeklár, Z. *Adv. Inorg. Biochem.* **1994**, *9*, 123−172.
(12) Gampp, H.; Zuberbühler, A. D. *Met. Ions Biol. Syst.* **1981**, *12*, 133−189.
(13) *Bioinorganic Catalysis*; Reedijk, J., Ed.; Marcel Dekker: New York, 1993.
(14) *Bioinorganic Chemistry of Copper*; Karlin, K. D., Tyeklár, Z., Eds.; Chapman & Hall: New York, 1993.

10.1021/ic981066m CCC: $18.00
Published on Web 04/09/1999

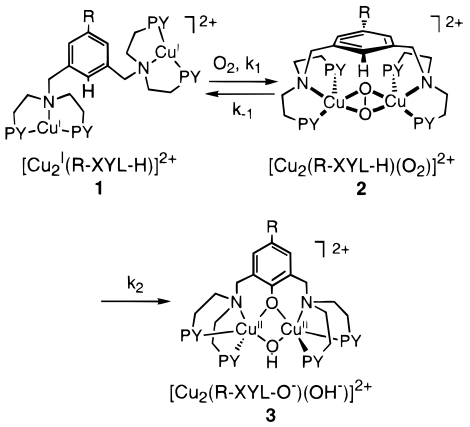

Figure 1. Model system for copper monooxygenases involving a dicopper(I)/O_2 mediated hydroxylation of the xylyl ligand aromatic substrate The scheme shown was deduced from stopped-flow kinetics studies in CH_2Cl_2 as solvent (PY = 2-pyridyl).

copper systems,[9,15] in focusing attention upon reversible O_2 binding (i.e., models for hemocyanins) and possible biomimics for tyrosinase. One such successful model system involves the reaction of molecular oxygen with the dinuclear complex $[Cu_2(H\text{-}XYL\text{-}H)]^{2+}$ (**1**), during which intramolecular ligand hydroxylation occurs quantitatively, giving $[Cu_2(H\text{-}XYL\text{-}O^-)(OH)]^{2+}$ (**3**) (Figure 1).[16,17] The peroxo complex $[Cu_2(H\text{-}XYL\text{-}H)(O_2)]^{2+}$ (**2**) could not be isolated, but its occurrence as an intermediate during this reaction was proven spectroscopically in a detailed stopped-flow kinetics study carried out in dichloromethane as reaction solvent.[18,19] Using a ligand−complex analogue $[Cu_2(NO_2\text{-}XYL\text{-}H)]^{2+}$ (with nitro substituent para to that position which is hydroxylated), we have shown that the corresponding intermediate $[Cu_2(NO_2\text{-}XYL\text{-}H)(O_2)]^{2+}$ (λ_{max} = 358, 435 nm) is long-lived at low temperatures,[19] and resonance Raman spectroscopic studies[20] indicate that this intermediate is a μ-η^2:η^2-peroxo bridged dicopper(II) species (Figure 1). Since the appearance of the initial description of the O_2 reaction of **1** as a copper monooxygenase model system,[17,21] other research groups have generated and described analogous reaction systems, employing xylyl analogue dicopper complexes.[22−33]

In this report, we describe further mechanistic inquiries into the reaction described in Figure 1, (i) by probing the use of another solvent, in particular, acetone, and (ii) by investigating the pressure dependence of the reaction. Variation of reaction medium can provide further insights into mechanism, due to differential stabilization of intermediates, binding of solvents in key labile coordination sites, etc. The application of high-pressure mechanistic studies to inorganic, bioinorganic, and organometallic chemistry has blossomed in the past decade;[34−36] a high-pressure kinetics investigation of O_2 binding to hemocyanin has been reported.[37] Determination of activation volumes ($\Delta V^{\ddagger}$) and construction of volume profiles can considerably aid or confirm the assignment of intimate mechanism on the basis of specific volume changes along a reaction coordinate.[34−36,38,39] Here, we describe a study of the reaction in Figure 1 at low temperatures under the influence of pressure and for the first time obtain the activation volumes for the individual reaction steps. This has not been possible in other work on the oxygenation of analogous dicopper(I) imine complexes where we were only able to measure activation volumes over the sum of all reaction steps.[40,41]

Experimental Section

Materials and Methods. Reagents and solvents used were of commercially available reagent quality. UV−vis spectra were measured on a Hewlett-Packard 8452 A spectrophotometer. ^{1}H NMR spectra were recorded on a Bruker DXP 300 AVANCE spectrometer. Elemental analyses were carried out at the University of Erlangen-Nürnberg. $[Cu_2(XYL\text{-}H)](PF_6)_2$ was synthesized according to the published procedure.[17]

High-Pressure Stopped-Flow Measurements. Reagent quality acetone either was used directly or was dried over Drierite (Aldrich) and immediately after distillation transferred into a glovebox (Braun, Garching, Germany (dioxygen and water content less than 1 ppm)). Solutions of complexes for the kinetics measurements were prepared in the glovebox and transferred with gastight syringes to the stopped-flow instrument. A dioxygen-saturated solution was prepared by bubbling dioxygen through acetone in a syringe (solubility of dioxygen in acetone at 25 °C = 0.0102 M).[42] Dilution was accomplished by mixing the solution with argon-saturated acetone. The effect of pressure was measured on a homemade high-pressure stopped-flow apparatus described elsewhere.[43] The high-pressure cell was modified by being surrounded with a thermostating mantle that allowed cooling down to −20 °C, and special glass syringes were used in the stopped-flow unit.

(15) Sorrell, T. N. *Tetrahedron* **1989**, *45*, 3−68.
(16) Karlin, K. D.; Dahlstrom, P. L.; Cozzette, S. N.; Scensny, P. N.; Zubieta, J. *J. Chem. Soc., Chem. Commun.* **1981**, 881−882.
(17) Karlin, K. D.; Gultneh, Y.; Hayes, J. C.; Cruse, R. W.; McKown, J. W.; Hutchinson, J. P.; Zubieta, J. *J. Am. Chem. Soc.* **1984**, *106*, 2121−2128.
(18) Cruse, R. W.; Kaderli, S.; Karlin, K. D.; Zuberbühler, A. D. *J. Am. Chem. Soc.* **1988**, *110*, 6882−6883.
(19) Karlin, K. D.; Nasir, M. S.; Cohen, B. I.; Cruse, R. W.; Kaderli, S.; Zuberbühler, A. D. *J. Am. Chem. Soc.* **1994**, *116*, 1324−1336.
(20) Pidcock, E.; Obias, H. V.; Zhang, C. X.; Karlin, K. D.; Solomon, E. I. *J. Am. Chem. Soc.* **1998**, *120*, 7841−7847.
(21) Karlin, K. D.; Dahlstrom, P. L.; Cozzette, S. N.; Scensny, P. M.; Zubieta, J. *J. Chem. Soc., Chem. Commun.* **1981**, 881.
(22) Sorrell, T. N.; Vankai, V. A.; Garrity, M. L. *Inorg. Chem.* **1991**, *30*, 207−210.
(23) Casella, L.; Gullotti, M.; Pallanza, G.; Ligoni, L. *J. Am. Chem. Soc.* **1988**, *110*, 4221−4227.
(24) Gelling, O. J.; van Bolhuis, F.; Meetsma, A.; Feringa, B. L. *J. Chem. Soc., Chem. Commun.* **1988**, 552−554.
(25) Gelling, O. J.; Feringa, B. L. *J. Am. Chem. Soc.* **1990**, *112*, 7599−7604.
(26) Menif, R.; Martell, A. E.; Squattrito, P. J.; Clearfield, A. *Inorg. Chem.* **1990**, *29*, 4723−4729.
(27) Shen, C.-Y.; Hu, M.-F.; Luo, Q.-H.; Shen, M.-C. *Transition Met. Chem.* **1995**, *20*, 634−635.
(28) Ghosh, D.; Lal, T. K.; Ghosh, S.; Mukherjee, R. *Chem. Commun.* **1996**, 13−14.
(29) Alzuet, G.; Casella, L.; Villa, M. L.; Carugo, O.; Gullotti, M. *J. Chem. Soc., Dalton Trans.* **1997**, 4789−4794.
(30) Mahapatra, S.; Kaderli, S.; Llobet, A.; Neuhold, Y.-M.; Palanché, T.; Halfen, J. A.; Young, V. G., Jr.; Kaden, T. A.; Que, L., Jr.; Zuberbühler, A. D.; Tolman, W. B. *Inorg. Chem.* **1997**, *36*, 6343−6356.
(31) Casella, L.; Gullotti, M.; Radaelli, R.; Di Gennaro, P. *J. Chem. Soc., Chem. Commun.* **1991**, 1611−1612.
(32) Casella, L.; Monzani, E.; Gullotti, M.; Cavagnino, D.; Cerina, G.; Santagostini, L.; Ugo, R. *Inorg. Chem.* **1996**, *35*, 7516−7525.
(33) Sayre, L. M.; Nadkarni, D. *J. Am. Chem. Soc.* **1994**, *116*, 3157−3158.
(34) Drljaca, A.; Hubbard, C. D.; van Eldik, R.; Asano, T.; Basilevsky, M. V.; Le Noble, W. J. *Chem. Rev.* **1998**, *98*, 2167−2289.
(35) van Eldik, R.; Merbach, A. E. *Comments Inorg. Chem.* **1992**, *12*, 341−378.
(36) van Eldik, R.; Asano, T.; Le Noble, W. J. *Chem. Rev.* **1989**, *89*, 549−688.
(37) Projahn, H.-D.; Schindler, S.; van Eldik, R.; Fortier, D. G.; Andrew, C. R.; Sykes, A. G. *Inorg. Chem.* **1995**, *34*, 5935−5941.
(38) Goldstein, S.; Czapski, G.; van Eldik, R.; Cohen, H.; Meyerstein, D. *J. Phys. Chem.* **1991**, *95*, 1282−1285.
(39) Zhang, M.; van Eldik, R.; Espenson, J. H.; Bakac, A. *Inorg. Chem.* **1994**, *33*, 130−133.
(40) Becker, M.; Schindler, S.; van Eldik, R. *Inorg. Chem.* **1994**, *33*, 5370−5371.
(41) Ryan, S.; Adams, H.; Fenton, D. E.; Becker, M.; Schindler, S. *Inorg. Chem.* **1998**, *37*, 2134−2140.
(42) Lühring, P.; Schumpe, A. *J. Chem. Eng. Data* **1989**, *34*, 250−252.
(43) van Eldik, R.; Gaede, W.; Wieland, S.; Kraft, J.; Spitzer, M.; Palmer, D. A. *Rev. Sci. Instrum.* **1993**, *64*, 1355−1357.

Single wavelength absorbance time traces were measured under pseudo-first-order conditions, and data fitting was performed with the software KINFIT (On-line Instrument Systems, Bogart, GA) and Igor Pro (WaveMetrics, Lake Oswego).

Variable-Temperature Stopped-Flow Measurements. Acetone (Uvasol, Merck) was used without further purification. The following linear equation describing the solvent thermal expansion was used to calculate the solution concentrations at various temperatures: ρ (g/mL) $= -1.1248 \times 10^{-3}T$ (K) $+ 1.1218$.[30]

All kinetics experiments were carried out using a variable-temperature stopped-flow unit (modified SFL-21, Hi-Tech-Scientific) combined with a photodiode-array spectrometer. Further details, also concerning preparation and handling of solutions, were as described previously.[44] Three series of experiments were performed with 0.753, 0.315, and 0.119 mM complex concentrations (at room temperature) between -90.2 and $+23.7$ °C. The initial oxygen concentration was 5.106 mM for all three series.

A total of 151 individual runs were performed. Data collection times were varied between 0.7 and 913 s. All data were pretreated by factor analysis, and individual rate constants were calculated by numerical integration of the appropriate rate laws using the self-developed Kinfit (Basic PDS) and Serkin (Matlab) programs. In most cases, the data could be described by two relaxations, which were converted into the correct model containing k_1, k_{-1}, and k_2 (see Figure 1). To this end the rate constant k_{-1} was manually changed so that the spectrum of the intermediate, which is only fully formed at low temperature, remained constant. We could successfully analyze 84 measurements in the range -64 to -0.2 °C and use them for the final activation parameter calculations. The set of data used for the final calculations included neither the room temperature runs (very little adduct formation) nor those at very low temperatures where excessive photochemical interference was observed.

Activation parameters for k_1, k_{-1}, and k_2 were obtained through analysis either with the Microsoft Excel 97 linear regression tool or with a nonlinear least-squares regression Matlab program.

Results and Discussion

Solvent Media for Reaction. For technical reasons, the simple extension of the previous detailed kinetic study[19,45] in dichloromethane solvent to conditions of high pressure proved impossible. Methanol, a good solvent for high-pressure studies,[40] was also found not to be suitable for the present system. Experiments in MeOH, carried out by mixing $[Cu(CH_3CN)_4]$-PF_6 with the ligand in situ, followed by oxygenation, were found to be considerably complicated by the presence of even small amounts of acetonitrile, with its known strong binding to, and stabilization of, copper(I).[46,47] The use of synthetically generated $[Cu_2(H\text{-}XYL\text{-}H)](PF_6)_2$ (**1-(PF$_6$)$_2$**) (prepared free of MeCN)[17] in MeOH solvent was thwarted by poor solubility; synthetically changing the anion to perchlorate did not help. Propionitrile was also considered as a solvent for **1**/O_2 reactivity studies, because of its successful application in low-temperature oxygenation of copper(I) complexes of tris(2-pyridylmethyl)amine (TMPA), its quinolyl analogues, and dinucleating analogues.[44,48,49] However, **1-(PF$_6$)$_2$** does not show intramolecular hydroxylation in EtCN, precluding its use as a reaction medium for further studies.

Acetone has also been found to be a good solvent for the study of reaction of O_2 complexes with copper(I) complexes,[41,50] and in certain cases it stabilizes and favors the formation of dioxygen adducts in comparison to analogous reactions studied in propionitrile.[50] **1-(PF$_6$)$_2$** is very soluble in acetone; thus the situation was amenable to high-pressure kinetics studies. The basic dinuclear structure and presence of **1** in solution is retained here, but the presence of altered structures or conformations is needed to fully explain the kinetic behavior in acetone, vide infra. Via either synthetic (at low or moderate solution concentrations) or spectroscopic UV−vis observation, oxygenation of **1-(PF$_6$)$_2$** in acetone solvent does afford the same product as in CH_2Cl_2, namely, **3** (Figure 1).

Complex $[Cu_2(H\text{-}XYL\text{-}H)](PF_6)_2$ (1-(PF$_6$)$_2$) in Acetone. Copper(I) complexes often exhibit temperature-dependent dynamic behavior involving ligand switching or conformational changes.[19,51−55] Variable-temperature ^{1}H NMR measurements of $[Cu_2(R\text{-}XYL\text{-}H)]^{2+}$ (e.g., R = MeO, *t*-Bu, H, NO_2) complexes in CD_2Cl_2 solvent exhibit such behavior. The effects are R-dependent and affect the O_2 reaction kinetics.[19] Variable-temperature NMR spectra (+25 to −80 °C) of **1-(PF$_6$)$_2$** in acetone-d_6 (Figure S1)[56] indicate dynamic behavior, with averaged spectra at room temperature but lowering of the complex's local symmetry at reduced temperatures. The behavior, however, differs to some extent from that observed in CD_2Cl_2.[57] A detailed analysis has not been carried out, but we suggest that **1** may form dimer structures (either intra- or intermolecular) in solution, especially as the temperature is lowered. We have recently observed dimerization occurring in acetone solution for copper(I) complexes with tetradentate tris(2-pyridylmethyl)amine (TMPA) complexes;[58] and there are now many other examples where copper(I) complexes in conjunction with tridentate or tetradentate nitrogen donors adopt dimer structures in solution or the solid state (confirmed by X-ray diffraction), via mutual sharing of one donor (e.g., a pyridine) of the polydentate ligand with the other copper ion center.[51,55,59−61]

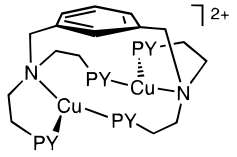

(44) Karlin, K. D.; Wei, N.; Jung, B.; Kaderli, S.; Niklaus, P.; Zuberbühler, A. D. *J. Am. Chem. Soc.* **1993**, *115*, 9506−9514.
(45) Cruse, R. W.; Kaderli, S.; Meyer, C. J.; Zuberbühler, A. D.; Karlin, K. D. *J. Am. Chem. Soc.* **1988**, *110*, 5020−5024.
(46) Jardine, F. H. *Adv. Inorg. Chem. Radiochem.* **1975**, *17*, 115−163.
(47) Hathaway, B. J. In *Comprehensive Coordination Chemistry*; Wilkinson, G., Ed.; Pergamon: New York, 1987; Vol. 5, pp 533−774.
(48) Lee, D.-H.; Wei, N.; Murthy, N. N.; Tyeklár, Z.; Karlin, K. D.; Kaderli, S.; Jung, B.; Zuberbühler, A. D. *J. Am. Chem. Soc.* **1995**, *117*, 12498−12513.
(49) Karlin, K. D.; Kaderli, S.; Zuberbühler, A. D. *Acc. Chem. Res.* **1997**, *30*, 139−147.
(50) Karlin, K. D.; Lee, D.-H.; Kaderli, S.; Zuberbühler, A. D. *Chem. Commun.* **1997**, 475−476.
(51) Mealli, C.; Arcus, C. A.; Wilkinson, J. L.; Marks, T. J.; Ibers, J. A. *J. Am. Chem. Soc.* **1976**, *98*, 711−718.
(52) Coggin, D. K.; Gonzalez, J. A.; Kook, A. M.; Stanbury, D. M.; Wilson, L. J. *Inorg. Chem.* **1991**, *30*, 1115−1125.
(53) Tyeklár, Z.; Jacobson, R. R.; Wei, N.; Murthy, N. N.; Zubieta, J.; Karlin, K. D. *J. Am. Chem. Soc.* **1993**, *115*, 2677−2689.
(54) Jacobson, R. R. Ph.D. Thesis, State University of New York at Albany, 1989.
(55) Carrier, S. M.; Ruggiero, C. E.; Houser, R. P.; Tolman, W. B. *Inorg. Chem.* **1993**, *32*, 4889−4899.
(56) See Supporting Information.
(57) For $[Cu_2(H\text{-}XYL\text{-}H)](PF_6)_2$ in acetone-d_6, resonances assigned to $-CH_2CH_2-$ methylene protons between pyridyl rings and alkylamine nitrogen are two broad but distinctive singlets at room temperature (δ, 3.1, 3.3 ppm) but broaden and then split into distinctive multiplets (δ, ∼2.8−3.4 ppm) upon lowering the temperature; the xylyl benzylic protons are a singlet which remains sharp, but shift from $\delta = 3.8$ to 4.1 ppm (+25 → −80 °C). For $[Cu_2(H\text{-}XYL\text{-}H)](PF_6)_2$ in CD_2Cl_2 the $-CH_2CH_2-$ protons are a broad doublet at +25 °C, while broadening and splitting similar to that in acetone-d_6 occurs as the temperature is lowered; but unlike for acetone-d_6, the xylyl benzylic proton resonance broadens significantly at −80 °C, as does also the 6-pyridyl proton resonance.

Scheme 1

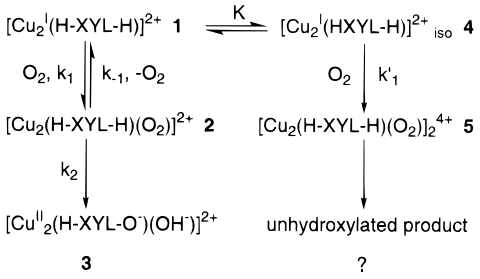

We suggest this possibility here, occurring possibly in an *intra*molecular fashion (as shown) and/or via similar *inter*molecular "bridging" of pyridyl donors.

Variable-Temperature Stopped-Flow Measurements in Acetone. The data obtained in previous studies[18,19] performed in CH_2Cl_2 are explained with two exponentials with a simple model including a pseudo-first-order rate constant k_1, first order in **1** and in O_2 (in large excess), followed by a fast irreversible step, described by first-order rate constant k_2 (left part of Scheme 1). In the present study with acetone as solvent, the same reaction scheme was considered.

At low temperatures the formation of the intermediate **2** is nearly complete, so that k_{-1} is irrelevant. The spectrum of **2** shows typical absorption bands at 360 nm ($\epsilon > 14\,000$ M^{-1} cm^{-1}) and at 440 nm ($\epsilon \approx 4500$ M^{-1} cm^{-1}), assigned to ligand-to-Cu(II) charge-transfer absorptions, and there is an isosbestic point at about 420 nm. However, at higher temperatures, it was necessary to consider k_{-1} since the intermediate **2** is only partially formed. Thus a first-order rate constant k_{-1} was refined for each individual run from −34 to −0.2 °C until the calculated adduct spectrum goes through the isosbestic point found at low temperature.

Whereas the Eyring plots of k_{-1} and k_2 are linear (Figure 2) and allow the determination of the activation parameters ΔH and ΔS (Table 1), that of k_1 (Figure 2; referred to as $k_{1,obs}$) is peculiar. First, it is not linear with $1/T$, and additionally, it is concentration dependent below −28 °C. This behavior is unexpected with regard to the measurements previously undertaken in CH_2Cl_2.[19] To explain the first aspect we have to postulate that in a fast pre-equilibrium an isomerization process of $[Cu_2(H\text{-}XYL)]^{2+}$ takes place, to give $[Cu_2(H\text{-}XYL)]^{2+}{}_{iso}$ (**4**) (Scheme 1). This latter species could well be the alternative internally dimerized structure described above, then assumed to have a subdued reactivity toward O_2. The constant K is the associated equilibrium constant, Scheme 1. Thus at moderately low temperatures the observed rate constant $k_{1,obs}$ is given by

$$k_{1,obs} = k_1/(1 + K)$$

which describes the situation where **1** is the predominantly reacting species. Analysis of the data taken in the temperature range −0.2 to −28 °C for the three concentrations and those of the series with the lowest concentration down to −64 °C gives the thermodynamic and activation parameters for K and k_1 (Table 1). The quality of the fitting of data to these equations

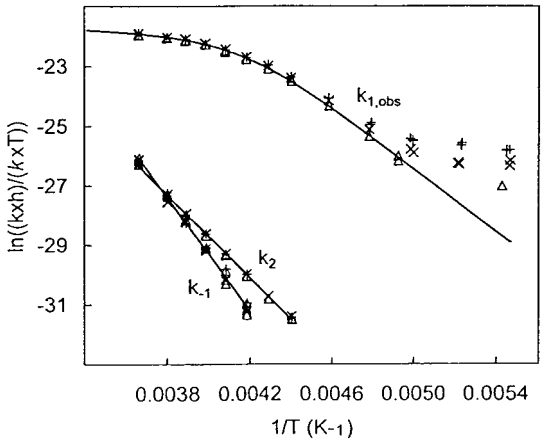

Figure 2. Eyring plots for for $k_{1,obs}$, k_{-1}, and k_2: k, Boltzmann constant; h, Planck constant. **1-(PF_6)$_2$**: (+) 0.75 mM, (△) 0.119 mM, (×) 0.315 mM, all at room temperature; (—) calculated curves.

can be seen from Figure 2. The temperature dependence is thus described by the following relation:

$$\ln[(k_{1,obs}h)/(kT)] = -\Delta H_1/(RT) + \Delta S_1/R - \ln\{1 + \exp[(-\Delta H_K/(RT)) + (\Delta S_K/R)]\}$$

At the lowest temperatures, **4** is formed almost exclusively and then its own reactivity becomes significant as **1** is depleted. At those temperatures where the calculation gives a concentration-dependent $k_{1,obs}$, the fit of the first relaxation was in all cases improved by taking a kinetic model with an additional third-order rate constant k'_1 (second order in $[Cu_2(H\text{-}XYL)]^{2+}$ ($k'_1 \sim 20\,000$ M^{-2} s^{-1}, at $T = -82$ °C). Thus, the right part of Scheme 1 describes this situation, the path in which two molecules of **4** react with O_2 to give the tetranuclear species $[Cu_2(H\text{-}XYL)(O_2)]_2^{4+}$ (**5**).

A final point in consideration of the stopped-flow variable-temperature study is the interference from the strong photochemistry (using the diode-array white light source) of **1**. Below −50 °C, a photochemical temperature-independent term becomes relevant when analyzing the behavior of the rate constant k_2. This behavior was also observed in dichloromethane as solvent.[19] Thus, only the thermal reaction part from −0.2 to −46 °C was considered for the determination of the activation parameters of k_2, as indicated in Figure 2.

From the data summarized in Table 1, it can be seen that the kinetic and thermodynamic parameters for the reaction of **1** with dioxygen are comparable to those previously observed in dichloromethane.[19] As is generally seen,[19,49] a difference in enthalpy is accompanied by a corresponding compensation in entropy, leading to overall rather similar rate constants in the temperature range studied. The formation of the intermediate dioxygen complex **2** (peroxo−dicopper(II) species with μ-η^2:η^2 structure)[20] is reversible, and its spectroscopic observation at lower temperatures is aided by favorable relative rates of formation of **2** and its decomposition to **3**, e.g., $k_1[O_2] > k_2$. As before, formation of **2** (k_1) occurs with very low activation enthalpy but with a large negative activation entropy, the latter being expected for O_2 binding without concomitant release of solvent from the metal center. The process described by k_1 must be a composite rate constant since it is unlikely that O_2 would bind to both copper ions simultaneously.[19] In fact, in a study of O_2 binding with a closely related ligand complex shown below, two O_2-bound intermediates (one observed spectroscopically, and a $Cu-O_2\cdots Cu$ superoxo complex inferred) precede forma-

(58) Karlin, K. D., and co-workers, unpublished results.
(59) Sorrell, T. N.; Borovik, A. S. *J. Am. Chem. Soc.* **1987**, *109*, 4255−4260.
(60) Sorrell, T. N.; Pigge, F. C.; White, P. S. *Inorg. Chim. Acta* **1993**, *210*, 87−90.
(61) Wei, N.; Murthy, N. N.; Tyeklár, Z.; Karlin, K. D. *Inorg. Chem.* **1994**, *33*, 1177−1183.
(62) Jung, B.; Karlin, K. D.; Zuberbühler, A. D. *J. Am. Chem. Soc.* **1996**, *118*, 3763−3764.

Table 1. Thermodynamic and Activation Parameters for the Higher Temperature Part of the Reaction of **1** with O_2 in Acetone

	T range, °C [data points]	calcd constants (−20 °C)	ΔH, kJ/mol	ΔS, J/(K mol)	high-pressure rate constants [pressure, MPa] (−20 °C)	$\Delta V^{\ddagger}$, cm^3/mol
K, M^{-1}	−64.2 to −0.2 [69]	1.06×10^3	-42.3 ± 0.4	-176 ± 2		
k_1, $M^{-1}\,s^{-1}$	−64.2 to −0.2 [69]	1.58×10^3	2.1 ± 0.7	-174 ± 3	1210 ± 64 [20]	-15 ± 2.5
					1570 ± 118 [60]	
		2.53×10^3 [a]	8.2 ± 0.3[a]	-146 ± 1[a]	2240 ± 247 [100]	
$k_{-1}\,s^{-1}$	−34.3 to −0.2 [60]	1.50	80.3 ± 0.8	77 ± 3	3.35 ± 0.38 [20]	$+4.4 \pm 0.5$
					3.01 ± 1.17 [60]	
		7.76[a]	70 ± 1[a]	50 ± 6[a]	2.82 ± 1.10 [100]	
k_2, s^{-1}	−46.2 to −0.2 [77]	2.57	58.2 ± 0.2	-5.8 ± 0.9	3.34 ± 0.15 [20]	-4.1 ± 0.7
					3.66 ± 0.70 [60]	
		3.77[a]	50 ± 1[a]	-35 ± 2[a]	3.88 ± 0.24 [100]	

[a] In CH_2Cl_2 solvent, from ref 19.

tion of the μ-η^2:η^2-peroxodicopper(II) product $[(N4)Cu_2(O_2)]^{2+}$.[62]

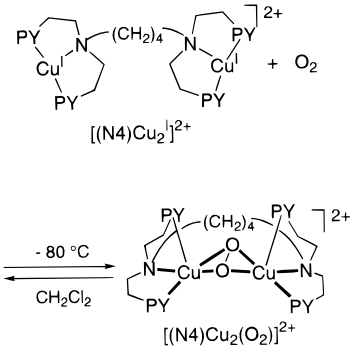

As discussed, explanation of the kinetics of the **1**/O_2 reaction in acetone requires postulating additional side reactions which become important at low temperature, Scheme 1. The kinetics data support the formation of the tetranuclear species **5** formed from an isomer of **1**, $[Cu_2(H\text{-}XYL)]^{2+}{}_{iso}$ (**4**), the nature of which is discussed above. In fact, we previously also presumed the existence of such a species **5** for the reaction studies carried out in dichloromethane.[19] Therefore, for reactions at higher concentrations (especially under benchtop synthetic conditions, i.e., $> \sim 10^{-3}$ M), this tetranuclear species was suggested to lead to the observed minor product $[Cu^{II}_2(H\text{-}XYL\text{-}H)(OH)]^{3+}$, which possesses oxidized copper(II), but in which the ligand is not hydroxylated. Under still quite other reaction conditions (in dimethylformamide/water), the kinetics/spectroscopic study implicated a tetranuclear hydroperoxo complex, which did lead to H-XYL-H ligand hydroxylation.[45] We have not further examined whether species **5** in acetone leads to **3** or some unhydroxylated product, Scheme 1.

High-Pressure Studies. At room temperature it is not possible to observe the formation of a peroxo−copper complex intermediate **2**. To study the pressure dependence of the reversible formation of **2**, it was therefore necessary to perform the investigation at reduced temperatures. This was accomplished by using a modified high-pressure stopped-flow instrument. Measurements were performed under pseudo-first-order conditions, and absorbance time traces were recorded at single wavelengths at −20 °C and pressures up to 100 MPa. An excellent fit to the sum of two exponential functions was possible, giving the same two rate constants at different wavelengths. Data obtained at the absorption maximum for the intermediate **2** (360 nm) were used thereafter. In a plot of the observed rate constants τ_1 and τ_2 vs the dioxygen concentration, a clear dependence of both rate constants was observed together with an intercept, as shown in Figure 3.[63] The reason for that

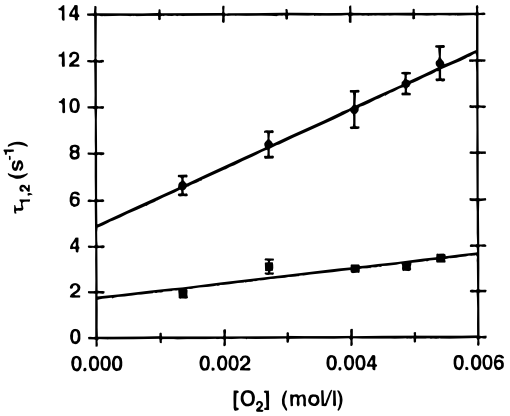

Figure 3. Plot of the observed rate constants τ_1 and τ_2 vs the dioxygen concentration at 600 MPa: (●) τ_1; (■) τ_2.

lies in the fact, that the three rate constants k_1, k_{-1}, and k_2 are very similar under the experimental conditions employed in the high-pressure part of this study. The favorable decomposition of intermediate **2** to give product **3** precludes conditions where **2** is fully formed; thus the maximum absorbance for the peroxo complex is never reached. Therefore, it is not possible to use the usual simplifications for data treatment, such as an assumption of a "fast pre-equilibrium" or "steady state" treatment. Instead it is necessary to use the exact results from solving the appropriate differential equations.[64] For a reversible pseudo-first-order reaction with a consecutive irreversible reaction, eq 1 is obtained.

$$\tau_{1/2} = \frac{1}{2}\left\{(k_1[O_2] + k_{-1} + k_2) \pm \sqrt{(k_1[O_2] + k_{-1} + k_2)^2 - 4k_1[O_2]k_2}\right\} \quad (1)$$

The dependence on the dioxygen concentration should lead to a nonlinear dependence of τ_1 and τ_2. That this is not the case (as can be seen in Figure 3) arises from the fact that the solubility of dioxygen in acetone is quite low and therefore the concentration range of dioxygen is not large enough to allow observation of the curvature; the high-concentration region where k_1, k_{-1}, and k_2 separate cannot be reached. To obtain the three rate constants k_1, k_{-1}, and k_2, they need to be extracted from eq 1.

(63) The observed intercepts in the plots for τ_2 vs dioxygen concentration (Figure 3) and the plot of $\tau_1\tau_2$ vs dioxygen concentration (Figure 5, Supporting Information) are not in accord with eqs 1 and 3. This arises from the presence of a very slow concurrent reaction which we could not better characterize. Efforts to include this other reaction and mathematically eliminate the intercept did not lead to significant changes of the values for the activation volumes in the range of error.

(64) Espenson, J. H. *Chemical Kinetics and Reaction Mechanisms*, 2nd ed.; McGraw-Hill: New York, 1995.

The relationship between the sum and the product of the measured rate constants τ_1 and τ_2, the dioxygen concentration, and k_1, k_{-1}, and k_2 is shown in eqs 2 and 3.

$$\tau_1 + \tau_2 = \frac{1}{2}\left\{(k_1[O_2] + k_{-1} + k_2) + \sqrt{(k_1[O_2] + k_{-1} + k_2)^2 - 4k_1[O_2]k_2}\right\} + \frac{1}{2}\left\{(k_1[O_2] + k_{-1} + k_2) - \sqrt{(k_1[O_2] + k_{-1} + k_2)^2 - 4k_1[O_2]k_2}\right\} = k_1[O_2] + k_{-1} + k_2 \quad (2)$$

$$\tau_1\tau_2 = \frac{1}{2}\left\{(k_1[O_2] + k_{-1} + k_2) + \sqrt{(k_1[O_2] + k_{-1} + k_2)^2 - 4k_1[O_2]k_2}\right\} \times \frac{1}{2}\left\{(k_1[O_2] + k_{-1} + k_2) - \sqrt{(k_1[O_2] + k_{-1} + k_2)^2 - 4k_1[O_2]k_2}\right\} = \frac{1}{4}(k_1[O_2] + k_{-1} + k_2)^2 - \frac{1}{4}\left(\sqrt{(k_1[O_2] + k_{-1} + k_2)^2 - 4k_1[O_2]k_2}\right)^2 = \frac{1}{4}(k_1[O_2] + k_{-1} + k_2)^2 - \frac{1}{4}(k_1[O_2] + k_{-1} + k_2)^2 - \frac{1}{4}(-4k_1[O_2]k_2) = k_1[O_2]k_2 \quad (3)$$

From the plot of the sum of τ_1 and τ_2 vs the dioxygen concentration shown in Figure S2[56] (eq 2), k_1 is obtained immediately. Constant k_2 is derived from the slope of the plot of the product $\tau_1\tau_2$ vs $[O_2]$ (eq 3) shown in Figure S3,[56] by dividing it by k_1.[63] Finally, k_{-1} is obtained from the intercept of the sum plot and subtraction of k_2. In this way, the three rate constants were calculated for all measured pressures. Rate constants at various pressures are given in Table 1. A plot of $\ln(k_1)$ vs pressure is shown in Figure S4,[56] and an activation volume $\Delta V^{\ddagger} = -15.0 \pm 2.5$ cm^3/mol was calculated from the slope. The activation volumes for the back (k_{-1}) and the consecutive reaction (k_2) were calculated in the same way, giving $\Delta V^{\ddagger} = +4.4 \pm 0.5$ cm^3/mol and $\Delta V^{\ddagger} = -4.1 \pm 0.7$ cm^3/mol (Table 1).

The strongly negative $\Delta S^{\ddagger}$ and $\Delta V^{\ddagger}$ values for the formation of peroxo−copper intemediate **2** support the concept of a highly structured transition state. The negative volume of activation can be thought of as a result of Cu−O_2 bond formation that is accompanied by electron transfer to produce **2**, where the change of formal oxidation state from copper(I) in **1** and reduction of O_2 to O_2^{2-} are expected to be accompanied by a significant volume collapse, partly due to intrinsic and solvational volume changes.[34] Similar effects have been described in situations of formal electron transfer for binding of aliphatic radicals to cobalt(II) and chromium(II) complexes (i.e., $M^{II}-R \rightarrow M^{III}-R^-$);[65,66] oxidative reactions in general exhibit significant negative volumes of activation.[67−69] The back reaction (k_{-1}; Scheme 1) is accompanied by positive values for $\Delta S^{\ddagger}$ and $\Delta V^{\ddagger}$, a consequence of a bond-breaking process. This is supported by the high activation enthalpy which is on the order of a copper−peroxo bond energy. Although, the actual reaction pathway must be more complicated (including probably a superoxo−Cu species, as mentioned above), the present study is the first where $\Delta V^{\ddagger}$ for the forward and back reactions could be measured for a process forming a dinuclear peroxo−dicopper species. This was not possible in earlier work where mechanisms of reactions of dinuclear copper Schiff base complexes with dioxygen were studied under the influence of pressure.[40,41] There, no peroxo complexes could be detected spectroscopically as intermediates and only a $\Delta V^{\ddagger}$ for the overall irreversible reaction to the product could be obtained.

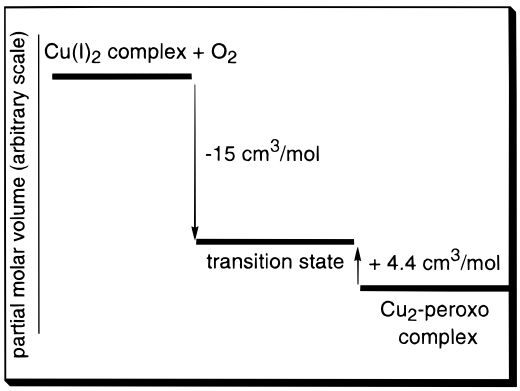

Figure 4. Volume profile for the reversible reaction of **1-(PF$_6$)$_2$** with dioxygen in acetone.

Thus, in the present case, a simplied volume profile can be constructed, as shown in Figure 4. The profile is unsymmetrical, and therefore a "late" (product-like) transition state is reached. The formation of the peroxo complex is accompanied by an overall volume collapse, a reaction volume of ∼20 cm^3/mol, and this value represents very well the bond formation of the complex with the dioxygen molecule.

The final irreversible step to the hydroxylated product **3** shows again a slightly positive value for $\Delta V^{\ddagger}$ and a small negative value for $\Delta S^{\ddagger}$ (Table 1). The small values combined with a considerable activation enthalpy indicate that hydroxylation is mainly governed by a bond-breaking process and little geometrical rearrangement, as discussed earlier[70] by explaining the observed reactivity with ideal positioning (i.e., proximity) of the peroxo group and xylyl substrate.

Taking into account that contributions of volume changes mainly arise from bond formation between the complex and O_2 (as discussed above), it seems appropriate to compare $\Delta V^{\ddagger}$ values obtained here with values obtained in studies on the Schiff base dicopper complexes mentioned, even though the latter pertain to the overall reaction. Thus, the activation volume $\Delta V^{\ddagger} = -15 \pm 2.5$ cm^3/mol for the formation of the peroxo complex **2** compares with $\Delta V^{\ddagger} = -21 \pm 1$ cm^3/mol for the macrocyclic complex $[Cu_2(mac)(CH_3CN)_2]^{2+}$ (mac = a dinucleating Schiff base macrocylic ligand)[40] and $\Delta V^{\ddagger} = -9.5$

(65) van Eldik, R.; Gaede, W.; Cohen, H.; Meyerstein, D. *Inorg. Chem.* **1992**, *31*, 3695−3696.
(66) van Eldik, R.; Cohen, H.; Meyerstein, D. *Angew. Chem., Int. Ed. Engl.* **1991**, *30*, 1158−1160.
(67) Dücker-Benfer, C.; van Eldik, R.; Canty, A. J. *Organometallics* **1994**, *13*, 2412−2414.
(68) de Waal, D. J. A.; Gerger, T. I. A.; Louw, W. J.; van Eldik, R. *Inorg. Chem.* **1982**, *21*, 2002−2006.
(69) Venter, J. A.; Leipoldt, J. G.; van Eldik, R. *Inorg. Chem.* **1991**, *30*, 2207−2209.
(70) Karlin, K. D.; Tyeklár, Z.; Zuberbühler, A. D. In *Bioinorganic Catalysis*; Reedijk, J., Ed.; Marcel Dekker: New York, 1993; pp 261−315.

$\pm$ 0.5 cm^3/mol for $[Cu_2(H\text{-}BPB\text{-}H)(CH_3CN)_2]^{2+}$ (H-BPB-H = 1,3-bis[*N*-(2-pyridylethyl)formimidoyl]benzene).[41] Furthermore, a very comparable value of $\Delta V^{\ddagger} = -12.8 \pm 0.9$ cm^3/mol was obtained for the formation of a peroxo−diiron(III) complex from the reaction of O_2 with a diiron(II) complex; this was accompanied by a very negative value, $\Delta S^{\ddagger} = -121 \pm 3$ J mol^{-1} K^{-1}.[71]

Thus, it seems to be the general case that dinuclear copper(I) and probably iron(II) complexes are accompanied by large negative values for $\Delta V^{\ddagger}$ (and $\Delta S^{\ddagger}$), interpreted as involving rate-determining O_2 binding (as superoxo or peroxo, for two metals) and electron transfer, leading to a tightly bound, organized and contracted transition state. It is notable that, in the case of dinuclear dioxygen carrier proteins such as hemocyanin and hemerythrin (non-heme diiron), the volumes of activation are positive or close to zero,[37] thus contrasting significantly from the negative values seen for copper and iron model compounds. A somewhat similar situation is observed for overall entropy changes for O_2 binding to simple complexes versus metalloproteins. The expected signficant loss in translational entropy of O_2 binding to metal ions is observed in model compounds, but small or even positive $\Delta S°$ values are observed for hemocyanin, for example.[18,49] In proteins, accompanying tertiary structural conformational changes in the protein matrix are presumed to reverse the situation.

Summary and Conclusions

Kinetic mechanistic investigations on the reaction of **1** with dioxygen in acetone corroborate and deepen findings observed in previous studies carried out in dichloromethane solvent, on substituted xylyl dicopper(I) complexes **1**.[19] A low-activation initial binding (k_1; Scheme 1) of O_2 occurs, to reversibly produce the copper−dioxygen [peroxo−dicopper(II)] intermediate **2**, and this irreversibly undergoes a ligand-hydroxylation (k_2; Scheme 1) reaction affording final product **3**. The activation parameters for all steps (k_1, k_{-1}, and k_2) parallel those found for dichloromethane. In acetone, however, the chemistry and the analysis are complicated by an equilibrium of dicopper(I) complex **1** with a less reactive isomer form **4** (Scheme 1). At low temperatures and higher concentrations, **4** becomes significant, resulting in a side reaction. More importantly, the high-pressure studies carried out here for the first time lead to activation volume information, not just for the overall reaction **1** → **3** but for the individual steps involved. The overall $\Delta V^{\ddagger}$ observed is similar to that observed in imine-ligand dicopper(I) reactions with dioxygen, while the present study reveals that this value is similar to the first step itself, indicating that contributions from volume changes occur mainly from bond formation between precursor dicopper(I) complex and dioxygen. Thus, $\Delta V^{\ddagger}(k_1) = -15 \pm 2.5$ cm^3/mol for formation of **2** from **1**. Along with the large and negative $\Delta S^{\ddagger}(k_1)$ (=−174 $\pm$ 3 J/K mol), these data show how rate-determining O_2 binding proceeds through a contracted, tightly bound transition state. The activation volume data provided here (i.e., the aggregated values associated with k_1k_2/k_{-1}) can be compared and are similar to those observed for other copper(I)/dioxygen reactions, and even to those for diiron(II) complex reactions with O_2.

These studies contribute to the body of mechanistic information now available on reactions of reduced-metal ion reactions with dioxygen and further demonstrate the complementary insights which can be obtained through variable-pressure kinetic studies.

Acknowledgment. Financial support by the Swiss National Science Foundation and the Bundesamt für Bildung und Wissenschaft (COST D1) (T.A.K. and A.D.Z.) is gratefully acknowledged. K.D.K. thanks the National Institutes of Health (GM28962). M.B. and S.S. gratefully acknowledge financial support from the Deutsche Forschungsgemeinschaft and the Volkswagen-Stiftung. Furthermore they would like to thank Prof. Rudi van Eldik for his support of this work and Prof. André Merbach and Dr. Pascal Bugnon (University of Lausanne, Switzerland) for their assistance at the beginning of the high-pressure investigations.

Supporting Information Available: Variable-temperature ^{1}H NMR spectra of $[Cu_2(H\text{-}XYL\text{-}H)](PF_6)_2$ in acetone-d_6 (Figure S1), plots of $(\tau_1 + \tau_2)$ vs $[O_2]$ at various pressures (Figure S2), plots of $(\tau_1 \times \tau_2)$ vs $[O_2]$ at various pressures (Figure S3), and plot of $\ln(k_1)$ vs pressure (Figure S4). This material is available free of charge via the Internet at http://pubs.acs.org.

IC981066M

(71) Feig, A. L.; Becker, M.; Schindler, S.; van Eldik, R.; Lippard, S. J. *Inorg. Chem.* **1996**, *35*, 2590−2601.